Journal of Power Sources 243 (2013) 562–568

Contents lists available at SciVerse ScienceDirect

Journal of Power Sources

journal homepage: www.elsevier.com/locate/jpowsour

The effects of hydride chemistry, particle size, and void fraction on micro fuel cell performance

S. Eickhoff [a,b,*], C. Zhang [b], T. Cui [a]

[a] Department of Mechanical Engineering, University of Minnesota, 111 Church Street SE, Minneapolis, MN 55455, USA
[b] Honeywell International, Automation and Control Solutions Research Laboratory, Plymouth, MN 55441, USA

HIGHLIGHTS

- Hydrolysis reactions were performed at three particle sizes and void fractions.
- Void fraction and particle size strongly affect reaction rates.
- Void fraction and particle size do not impact reaction yields.
- Energy density of 1003 Wh L^{-1} was demonstrated—the highest reported to date.

ARTICLE INFO

Article history:
Received 5 April 2013
Received in revised form
26 May 2013
Accepted 28 May 2013
Available online 14 June 2013

Keywords:
Micro fuel cell
Chemical hydride
Water recovery
Void fraction
Particle size

ABSTRACT

This paper explores the effects of fuel chemistry and pellet configuration (void fraction, particle size) on MFC reaction rate and yield. Candidate hydrides were evaluated based on their suitability in a MFC using water vapor-driven hydrolysis, and lithium aluminum hydride ($LiAlH_4$) was selected for evaluation. Hydrogen evolution tests were performed in a hydrolysis reactor with three particle size distributions (5 μm, 20 μm, and 50 μm in mean diameter) and at three initial void fractions (86%, 71%, 43%). Void fraction and particle size are found to affect reaction rates, but have no impact on reaction yields (all were ~100%) within the range tested. Higher void fraction and smaller particle size are correlated with faster reaction rates.

Electrical discharge tests are performed on a MFC at a constant potential of 1.2 V at three particle sizes (5 μm, 20 μm, 50 μm) at a 32% initial void fraction. Tests in the MFC reveal the strong impact of particle sizes on reaction rates, and show that reaction rates decrease with increasing particle size. Reaction yields are lower (90–93%) in the MFC, which is attributed to a small hydrogen leak. The energy density of the MFC is 1003 Wh L^{-1}, the highest reported to date.

1. Introduction

Chemical hydrides have received considerable attention since their initial synthesis in the 1940s, as promising fuels for micro fuel cells (MFC) due to their superior hydrogen storage density relative to conventional hydrogen storage methods (e.g. compressed gas in cylinder) [1,2]. Although several mechanisms for releasing hydrogen from chemical hydrides have been explored, including thermal decomposition (thermolysis) and the water-hydride (hydrolysis) reaction, hydrolysis appears to be the most promising. Indeed, studies of hydride hydrolysis reactions with water vapor have demonstrated yields approaching unity at rates sufficient for MFCs [3–5]. Recently, the author [6,7] and others [8] reported "water-recovery" hydrogen generators, which recycle fuel cell-generated water and use it in the hydrolysis reaction, eliminating water as an onboard reactant. This innovation improves the theoretical energy density of the hydride by approximately 2×, as the water can be neglected in the energy density calculation because it is available for "free" from the fuel cell. Water recovery also simplifies fuel cell system design by eliminating water storage and handling components, and improves safety by delivering water as-needed, precluding a dangerous release of heat and hydrogen were the water and hydride to react in an uncontrolled manner.

MFCs using water-vapor hydrolysis and fuel cell water recovery were reported by the author [7,8] and others [9]; the MFC reported in a recent paper by this author [8] achieved an energy density of

* Corresponding author. Honeywell International, Automation and Control Solutions Research Laboratory, Plymouth, MN 55441, USA. Tel.: +1 763 954 2380; fax: +1 763 954 2504.
E-mail addresses: steven.eickhoff@honeywell.com, steveneickhoff@yahoo.com (S. Eickhoff).

0378-7753/$ – see front matter © 2013 Elsevier B.V. All rights reserved.
http://dx.doi.org/10.1016/j.jpowsour.2013.05.167

987 Wh L^{-1}, the highest reported to date. In the same paper, we suggest that further improvements in energy density are possible by optimizing the chemistry and fuel pellet configuration (void fraction, geometry, particle size and distribution, etc.), and that energy densities in excess of 2000 Wh L^{-1} may be possible in optimized MFCs discharged at a low power.

In the present work, we explore the effects of fuel chemistry and pellet configuration (void fraction, particle size, etc.) on MFC reaction rate and yield. These data will be used to support a modeling effort to improve MFC pellet design, and will be the subject of a future paper.

We start by surveying and selecting four candidate hydrides for experimental evaluation, using both conventional hydride selection criteria and the criteria we developed specifically for MFCs using vapor-driven hydrolysis reactions. The four candidate hydrides are then tested in a vapor-hydride reactor, and a single hydride is down-selected for further experimental work. For the down-selected hydride, the impact of void fraction and particle size on reaction rate and yield are then experimentally determined using a vapor-hydride reactor, followed by performance validation in a MFC.

2. Experimental

2.1. Hydride selection

Candidate hydrides were selected for preliminary experiments from the group of simple and complex hydrides identified by Kong et al. [3] by applying the selection criteria given by MacPherson [10]. These criteria include (1) maximum deliverable hydrogen, (2) ambient state and density, (3) storability, (4) delivery manageability and controllability of the reaction, (5) availability of the parent elements, (6) environmental impact, (7) recyclability, (8) heat of reaction, and (9) potential for economic feasibility.

Starting with the hydrides selected by Kong et al. based on MacPherson's criteria (Fig. 1), we narrow the list further by applying three additional requirements: (1) hydrogen release must occur via a hydrolysis reaction at near room temperature; (2) the hydride must react with water vapor; (3) the hydrolysis reaction must produce one mol of hydrogen per mol of water vapor consumed.

MgH_2 is eliminated because it does not react fast enough with water under normal ambient conditions due to formation of a $Mg(OH)_2$ surface layer which slows water transport to the unreacted core [12]. The borohydrides ($LiBH_4$ and $NaBH_4$) are eliminated because they do not react directly with water vapor [8]. The remaining four hydrides in Fig. 1 meet the additional criteria described above, and are selected for preliminary experiments. Table 1 contains the reaction equation, reactant and product energy density values for these four hydrides.

The reactant energy density values in Table 1 are calculated based on the energy content and volume of the hydride. The product energy density values are calculated based on the energy content of the hydride and volume of the hydride reaction products. For both parameters, the volume of the water reactant is neglected, as it is assumed that the water is recovered from the fuel cell. The energy values are calculated assuming stoichiometric reactions as shown in Table 1. Hydrogen is converted to electrical energy in a PEM fuel cell operating at 0.6 V, and that all other sources of inefficiencies and losses are negligible.

Product energy density is included in the analysis because all of the hydrides in Table 1 (except $NaAlH_4$) have smaller product than reactant energy densities. A smaller product energy density implies that the volume of the hydride is smaller than that of its reaction products, thus additional void space is required in the hydride to accommodate reaction product expansion. In volume-constrained applications (as is the case with the portable devices in which MFCs are used), this reduces the energy density of the hydride to that of its fully expanded reaction products. Thus, the smaller of the reactant or product energy densities is selected as the relevant basis of comparison.

Samples of each of the hydride listed in Table 1 are reacted in a vapor-hydrolysis reactor (Section 2.3). Based on the reaction yields observed in these experiments and the theoretical reactant and product energy density values (Table 1), we determine that $LiAlH_4$ has the highest practical energy density, and select it for further experiments to explore the effects of void fraction and particle size on reaction rate and yield.

Our selection of $LiAlH_4$ is somewhat surprising given the findings of Kong et al., who selected CaH_2 and LiH based on a similar analysis. A discussion of this discrepancy and a hypothesis for the differing results are presented in Section 3.1.

2.2. Hydride processing

The hydrides selected for testing were purchased from the Sigma Aldrich Chemical Company. Their catalog number, purity, and forms are summarized in Table 2.

The hydride powders were broken down to three sizes (5 μm, 20 μm, and 50 μm diameters) using a jet mill (Jet Pulverizer Co, Moorestown, NJ). Jet milling was chosen because it is capable of producing very small particles with narrow size distributions,

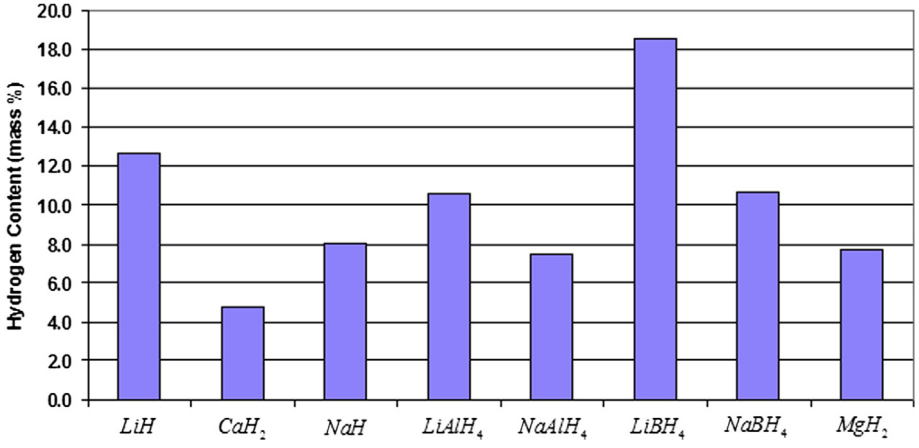

Fig. 1. Simple and complex hydrides and their formula hydrogen content selected for evaluation by Kong et al. by applying MacPherson's criteria.

Table 1
Reaction, reactant and product energy density, for hydrides meeting the selection criteria.

Hydride	Reaction	Formula H_2 content (mass%)	Specific energy (Wh kg)	Reactant energy density (Wh L^{-1})	Product energy density (Wh L^{-1})
LiH	$LiH + H_2O >> H_2 + LiOH$	12.7	4726	3875	2366
CaH_2	$CaH_2 + 2H_2O >> 2H_2 + Ca(OH)_2$	4.8	1783	3031	2238
$LiAlH_4$	$LiAlH_4 + 4H_2O >> 4H_2 + LiOH + Al(OH)_3$	10.6	3954	3626	3103
$NaAlH_4$	$NaAlH_4 + 4H_2O >> 4H_2 + NaOH + Al(OH)_3$	7.5	2779	2515	2927

while avoiding the excess heat production (which can decompose the hydride) and contamination that are typically associated with traditional milling processes (e.g. ball milling) [11].

For the hydride candidate selection tests (Section 3.1), ~0.5 g of hydride (5 μm size distribution) was loosely packed by hand into the fuel chamber, leaving sufficient free volume for reaction product expansion. The purpose of the selection tests is to determine the reaction yield, unconstrained by particle size or reaction product expansion (void fraction) limitations.

For all subsequent tests with the down-selected hydride ($LiAlH_4$), a hydraulic press (Carver, Wabash, IN) is used to compress the hydride to the desired void fraction. The desired mass of hydride for each test is divided in ten equal parts and pressed in stages, to minimize normal density gradients within the fuel chamber. Depending on the desired mass of hydride in the test, a force of up to 4000 lbs (~23,000 psi) is required to compress the hydride. Tests were performed with three particle size distributions (5 μm, 20 μm, and 50 μm diameters) and at three initial void fractions (86%, 71%, 43%).

2.3. Hydride reactor

A water-vapor-hydrolysis reactor was constructed as shown in Fig. 2, and it is similar in design to the reactor described by Kong et al. [3]. The reactor chamber is constructed from stainless steel and is hermetically sealed during the experiments. Hydrogen generated by the hydrolysis reaction is trapped inside the reactor, resulting in a pressure rise over time. The reaction rate and yield are determined based on the rate of pressure rise and final pressure in the reactor, respectively.

The hydride is contained in a cylindrical fuel chamber constructed from perforated stainless steel tubing. The fuel chamber is positioned on a load cell (Futek, Irvine, CA) above a pool of saturated salt solution. Filter paper soaked in the saturated salt solution and supported by a stainless steel screen is positioned around the fuel chamber. The saturated salt solution (a slush comprised of magnesium nitrate and distilled water) maintains a constant humidity boundary (nominally ~54.4% at 20 °C) around the fuel chamber. The load cell measures the mass of the hydride vs. time. The data is used to monitor reaction stoichiometry and water uptake by the reaction products.

The fuel chamber is weighed before and after filling with hydride. The exact mass of hydride loaded in the fuel chamber is determined by subtracting the empty mass of the fuel chamber from its fully loaded mass. All masses are measured with an analytical balance (Ohaus, Parsippany, NJ).

Table 2
Form, purity, and catalog numbers for selected hydrides.

Hydride	Form	Purity (%)	Catalog number
LiH	Powder	95	201049
CaH_2	Powder	95	208027
$LiAlH_4$	Powder	97	62420
$NaAlH_4$	Powder	93	685984

A temperature and humidity sensor (Sensiron, Los Angeles, CA) positioned between the filter paper and the fuel chamber monitors the temperature and humidity in the chamber. Similarly, a pressure sensor (Honeywell, Morristown, NJ) positioned near the top of the chamber monitors the pressure in the chamber. A movable plunger covers the fuel chamber and seals it from the surrounding environment during setup. The plunger is raised at the start of the test, allowing water vapor access to the fuel chamber.

The fuel chamber is filled with hydride inside a nitrogen-purged dry box and transported to the reactor in a sealed container. The fuel chamber is placed in the reactor and quickly covered with the plunger, to prevent the hydride from reacting with atmospheric water vapor while the reactor is assembled and purged. Once assembled, the reactor is purged with hydrogen for 30 min at 1000 sccm flow rate to eliminate atmospheric gases.

All experiments are carried out at 20 °C and 54.4% relative humidity. The pressure in the reactor starts at 1 atm, ultimately rising to 2–4 atm (depending on the amount and type of hydride) at the end of the test. Reaction rate and yield are calculated based on the rate of pressure rise and final pressure in the reactor, respectively.

2.4. Pellet evaluation in the MFC

Fuel pellet formulations are evaluated in the MFC as shown schematically in Fig. 3, and described in a previous paper [8]. The MFCs design and operating principle are summarized here for convenience.

The MFC is comprised of a hydrogen-air PEM fuel cell integrated with a self-regulating hydrogen generator. Hydrogen produced by

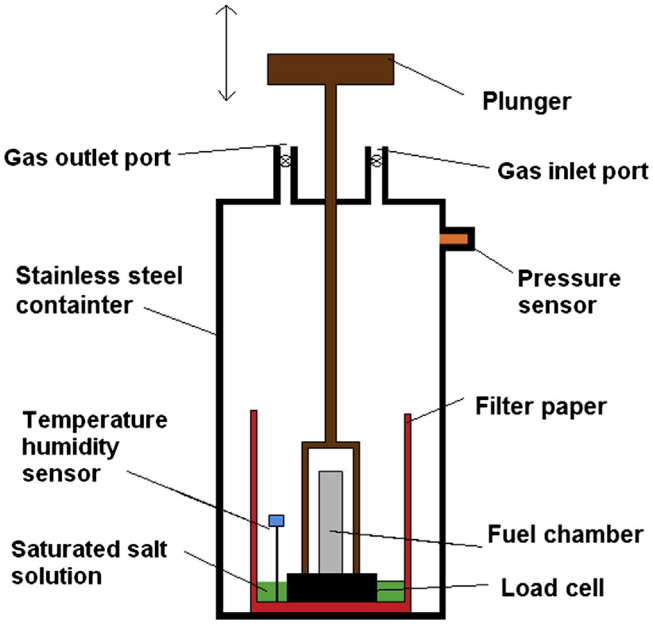

Fig. 2. Cross-section schematic of the vapor hydrolysis reactor.

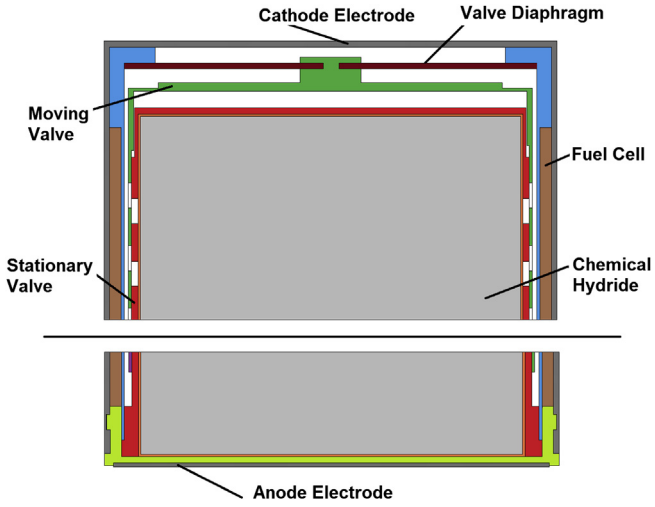

Fig. 3. Cross-section schematic of the MFC. The middle portion of the MFC is removed to more clearly show the top and bottom.

the hydrogen generator and oxygen from ambient air react at the fuel cell, generating electrical energy, water vapor, and waste heat. Water vapor generated at the fuel cell cathode back-permeates through the PEM and diffuses to the hydride, where it reacts to generate hydrogen.

The hydrogen generation rate is regulated by a pneumatic diaphragm valve which controls diffusive transport of water vapor from the fuel cells to the chemical hydride, based on the position of the diaphragm. The position of the diaphragm is determined by the pressure difference (ambient minus internal) across it. When an electrical load is placed on the MFC, hydrogen is consumed by the fuel cell, causing the internal pressure to drop and the diaphragm to deflect inward. This inward deflection opens the valve and allows water vapor to diffuse to and react with the hydride, generating hydrogen. When the load is removed hydrogen consumption stops, causing the internal pressure to rise and the diaphragm to deflect outward. This outward deflection closes the valve and stops water vapor transport to the hydride and hydrogen generation. The valve is partially open under normal operating conditions. It closes or opens completely under no-load or maximum-load conditions, respectively.

The MFC (Fig. 4.) has a 14 mm diameter and 50 mm height, and a volume of 7.7 cc. It has a nominal operating potential of 1.5 V and open circuit potential of ~1.9 V. Power output ranges from 0 to ~150 mW, depending on the operating potential and state of discharge.

Two circumferentially perforated bands in the metal case provide air access to the fuel cells. The cylindrical portion of the metal case functions as the MFC's cathode electrode, while the metal plate at the bottom functions as the anode.

MFC performance is characterized with a potentiostat running constant potential discharge tests in a temperature and humidity controlled ambient held at 20 °C and 54.4% relative humidity. Current and potential are monitored as a function of time until the MFC can no longer sustain the desired potential. Delivered energy and MFC energy density are calculated based on the potential and current data.

Prior to testing, the MFCs undergo a fueling process comprised of packing the desired fuel formulation in the fuel chamber (described in Section 2.2), followed by purging the fuel chamber for 5 min each with nitrogen and hydrogen gas at a flow rate of 100 sccm. The MFCs are then sealed with a fast-curing epoxy and placed under test.

Fig. 4. Photograph of the MFC next to quarter for reference.

3. Results and discussion

3.1. Hydride candidate evaluation

Hydrogen production profiles for the candidate hydrides are shown in Fig. 5.

High reaction yields were observed for all four hydrides, with CaH_2 and LiH achieving 96% and 94% yield respectively, and $LiAlH_4$ and $NaAlH_4$ both achieving ~100% yield. Reaction yields and practical energy density values for the four candidate hydrides are shown in Table 3. Yields are calculated based on the pressure rise in the reactor, and the reaction equations listed in Table 3, assuming complete (stoichiometric) reactions. Practical energy density is calculated for each hydride by taking the smaller of its reactant or product energy density and multiplying it by its reaction yield. Based on this analysis, $LiAlH_4$ has the highest practical energy density of the four hydrides.

The high observed reaction yields for all four-candidate hydrides is surprising for two reasons. First, for all of the hydrides except LiH,

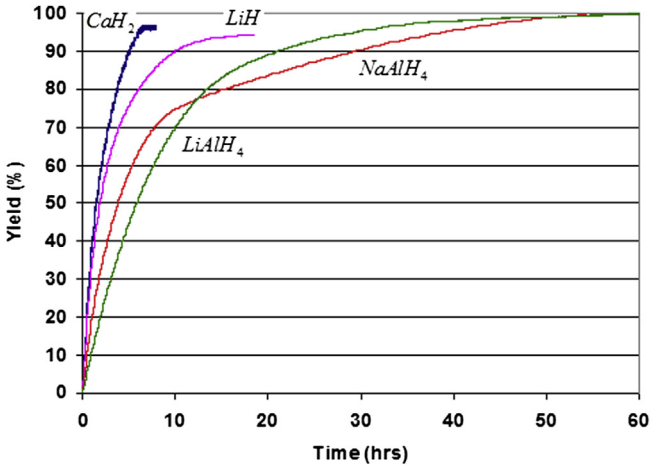

Fig. 5. Hydrogen production profiles for vapor hydrolysis reactions with candidate hydrides.

Table 3
Reaction, reactant and product theoretical energy density, reaction yield, and practical energy density for candidate hydrides.

Hydride	Reaction	Formula H_2 content (mass %)	Specific energy (Wh kg)	Reactant energy density (Wh L)	Product energy density (Wh L)	Reaction yield (%)	Practical energy density (Wh L)
LiH	$LiH + H_2O >> H_2 + LiOH$	12.7	4726	3875	2366	94	2224
CaH_2	$CaH_2 + 2H_2O >> 2H_2 + Ca(OH)_2$	4.8	1783	3031	2238	96	2149
$LiAlH_4$	$LiAlH_4 + 4H_2O >> 4H_2 + LiOH + Al(OH)_3$	10.6	3954	3626	3103	100	3103
$NaAlH_4$	$NaAlH_4 + 4H_2O >> 4H_2 + NaOH + Al(OH)_3$	7.5	2779	2515	2927	100	2515

yields are higher than the minimum purity (Table 2) specified by the manufacturer, indicating that the hydrides samples in our tests are very nearly pure. Second, we expected lower yields from $LiAlH_4$ and $NaAlH_4$ (~73% and ~49%, respectively) based on the results reported by Kong et al., however the yields for both reactions were ~100% [3].

We hypothesize the yields we observed, which are higher for two reasons. First, we use jet-milled hydrides with uniform and small (5 μm) particles, as opposed to the larger particle size and broad size distribution as-delivered by the manufacturer (Fig. 6) and used by Kong et al. in their experiments. The lower yields reported by Kong et al. may be a result of un-reacted hydride remaining in the core of the larger particles. Second, we use small hydride samples (~0.5 g) in our tests, and provide ample volume in the fuel chamber for reaction product expansion, resulting in reaction products that are dry, free-flowing, and non-agglomerated. This is opposed to reaction products described by Kong et al. as "hard solid masses", which may have limited yield by preventing water vapor access to the hydride in the interior of the pellet [3].

Hydrogen generation rates for the candidate hydrides in the (initial) linear region range from 1 e^{-5} mol s^{-1} for CaH_2 to 3.5 e^{-6} mol s^{-1} for $LiAlH_4$, corresponding to 1.2 W–0.4 W equivalent power, respectively, assuming that the hydrogen is converted to electricity in a fuel cell operating at 0.6 V. Reaction rates for all four candidate hydrides are adequate for the MFC, which has a peak power output of ~0.15 W.

Based on the practical energy density and initial reaction rates, $LiAlH_4$ is selected for further experiments to explore the effects of void fraction and particle size on reaction rate and yield.

3.2. Particle size effects

Hydrogen production profiles for $LiAlH_4$ at three particle sizes (5 μm, 20 μm, 50 μm diameters) at an 86% initial void fraction are shown in Fig. 7.

The tests were conducted at a high initial void fraction (86%) to minimize the impact of reaction product expansion on reaction rate and yield. The reaction yield for all three particle sizes was ~100%, indicating that particle size does not impact yield for the range of particle sizes tested. Reaction rates, however, were significantly impacted by particle size. Initial rates ranged from 3.5 e^{-6} mol s^{-1} for the 5 μm particle size, to 1.5 e^{-6} mol s^{-1} for the 50 μm particle size, corresponding to 0.4 W–0.17 W, respectively.

The slower reaction rate of the 50 μm particle size would begin to limit the maximum power output of the MFC (peak power of 150 mW) after only a few hours, thus in order to minimize the impact of the decreasing reaction rate with time, a smaller particle size is preferred.

There is, however, a lower limit to the preferred particle size from several perspectives. Fundamentally, as the particle size shrinks, so does the particle-to-particle spacing. Once this spacing is similar in magnitude to the mean free path of the gas, mass transfer rates begin to decrease as the transition from Fickian to Knudsen diffusion occurs. This transition occurs at ~1 μm particle size, for the conditions inside the MFC. In addition, current jet-mill technology has a lower particle size limit of ~0.5 μm, and has very low throughput at small particle sizes, impacting processing cost. Further, smaller particles are more reactive, and present a greater danger in case of an uncontrolled reaction with water. These factors must also be considered when selecting an optimal particle size for the MFC.

3.3. Void fraction

Hydrogen production profiles for hydrolysis reactions for $LiAlH_4$ at three initial void fractions (86%, 71%, 43%) with 5 μm particles are shown in Fig. 8.

The tests are conducted using 5 μm particles to minimize the effect of particle size on reaction rate and yield. The reaction yield for all three particle sizes was ~100%, indicating that void fraction does not impact yield for the range tested. This is expected, as the calculated final void fraction for even the lowest initial void fraction test is 34%, after accounting for reaction product expansion. For all three tests, however, the actual final void fraction was significantly

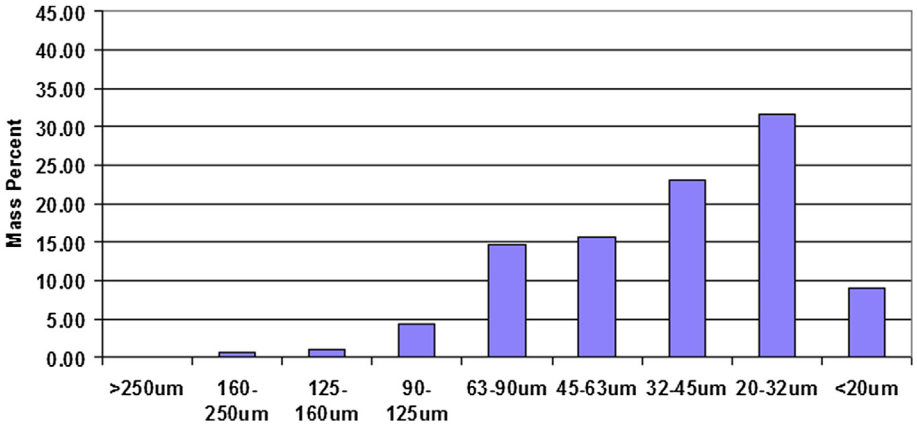

Fig. 6. Particle size distribution for $LiAlH_4$ as-received from the manufacturer.

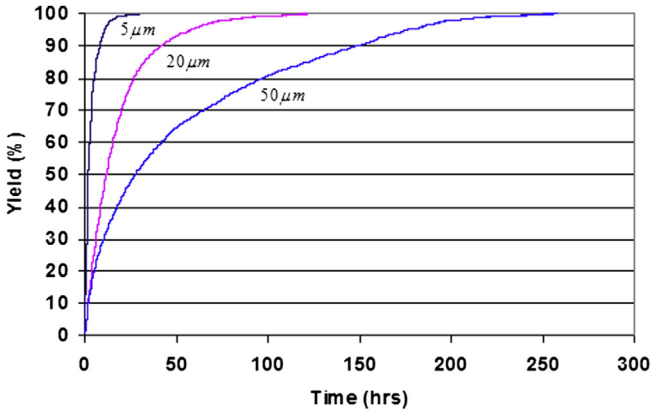

Fig. 7. Effects of particle size (5 μm, 20 μm, 50 μm) on reaction rate and yield in the hydrolysis reactor, at 86% initial void fraction.

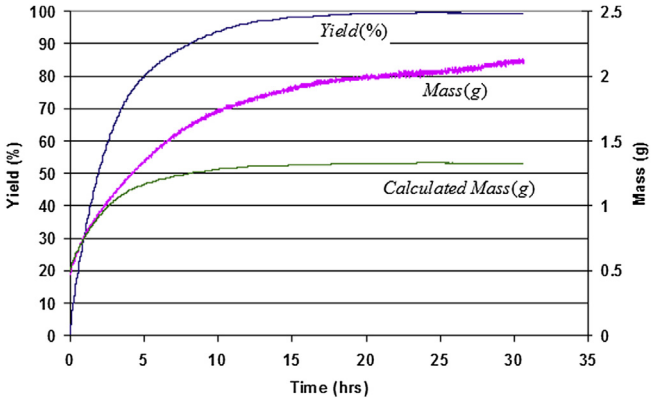

Fig. 9. Actual and calculated mass of hydride reaction products for 5 μm particles at an 86% initial void fraction.

lower than the calculated value, as determined by the final mass of the reaction products measured by the load cell. Fig. 9 shows the actual and calculated mass of the reaction products for the test conducted at an 86% initial void fraction.

The calculated mass is determined based on the measured yield assuming a stoichiometric reaction. During the first few hours of the test, the calculated and actual masses are in good agreement, however, at around three hours the masses begin to diverge, and the actual mass increases at a significantly higher rate than predicted by the reaction yield. The actual mass continues to rise even after the hydride reaction reaches completion.

Although there is no discussion in the literature of this phenomenon occurring for $LiAlH_4$, there is extensive literature concerning the LiH hydrolysis reaction, which also produces LiOH as a reaction product. The work of Maupoix et al. demonstrates that LiOH will form lithium hydroxide hydrate ($LiOH{\cdot}H_2O$) under the conditions present in the fuel chamber, giving a plausible explanation for the higher mass accumulation rate and final mass of the reaction products [5]. Although beyond the scope of the current paper, this side reaction, its impact on reaction rate and yield in MFCs will need to be considered when designing an optimal pellet configuration.

Reaction rates were significantly impacted by void fraction, although the exact effects are difficult to isolate given the confounding effects of the probable lithium hydroxide hydrate formation. Initial reaction rates ranged from 3.5 e^{-6} mol s^{-1} at 86% void fraction, to 3.3 e^{-6} mol s^{-1} at 43% void fraction, corresponding to 0.4 W–0.38 W, respectively. A lower void fraction is desirable as it proportionally increases energy density; however it also decreases the reaction rate. Further work will be required to understand the impact of initial void fraction and lithium hydroxide hydrate formation on reaction rate and energy density, and develop an optimal pellet configuration.

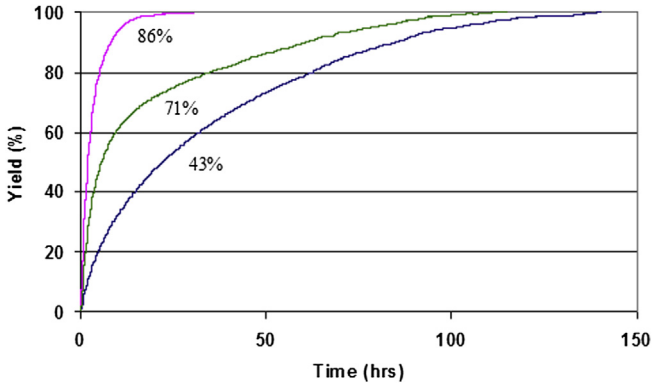

Fig. 8. Effects of initial void fraction (86%, 71%, 43%) on reaction rate and yield for lithium aluminum hydride with 5 μm particles.

3.4. Characterization in a MFC

Yield profiles for the MFC at 1.2 V constant potential discharge with $LiAlH_4$ at three particle sizes (5 μm, 20 μm, 50 μm) at a 32% initial void fraction are shown in Fig. 10.

Reaction yields for all three particle sizes are greater than 90%, with the 5 μm test yielding 93%, the 20 μm test yielding 91%, and the 50 μm test yielding 90%. These yields correspond to energy densities of 1003 Wh L^{-1}, 981 Wh L^{-1}, and 971 Wh L^{-1}, respectively, for the 7.7 cc MFC with 2.45 g of lithium aluminum hydride fuel (32% initial void fraction in the fuel chamber). 1003 Wh L^{-1} is the highest energy density reported to date for an MFC.

The lower yields of the tests in the MFC, as compared to the hydrolysis reactor, are likely attributed to the small hydrogen leak rates in the MFC, compared to the hermetically sealed hydrolysis reactor, which had no measurable leak rate. Progressively lower yields for the longer (larger particle sizes) tests support this hypothesis, as does the measured hydrogen leak rate of the empty MFC. The yield of the 5 μm test would likely be several percent higher, had the test not been cut short by a power failure.

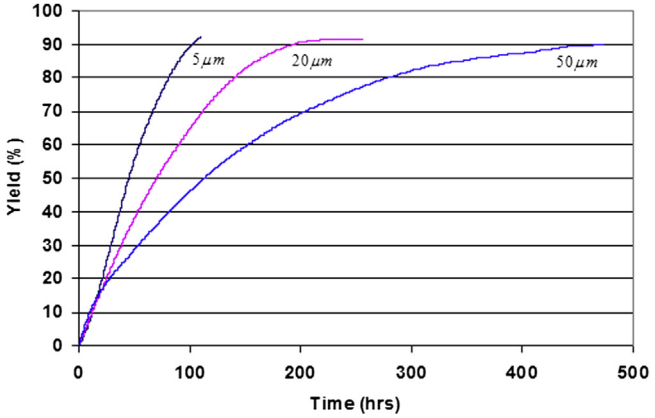

Fig. 10. Yield profiles at 1.2 V constant potential discharge for the MFC with lithium aluminum hydride at three particle sizes (5 μm, 20 μm, 50 μm) at a 32% initial void fraction.

As with the tests conducted in the hydrolysis reactor, the tests in the MFC show the strong impact of particle size on reaction rates, while reaction rates decrease with increasing particle size. Average reaction rates in the MFC were substantially lower ($\sim 5\times$) than in the hydrolysis reactor, as expected, due primarily to the added mass transfer resistance of the PEM in the fuel cell. The dominance of the mass transfer resistance of the PEM is clearly evident during the first 15 h of each test, during which the reaction rates were relatively independent of particle size, as indicated by the similar slopes of the yield curves. The curves diverge as the mass transfer resistance of the larger hydride particles begins to dominate the total resistance later in the tests.

4. Conclusion

We select LiH, CaH_2, $LiAlH_4$ and $NaAlH_4$ for preliminary evaluation in a vapor hydrolysis reactor. Although all of the hydrides tested had high reaction yields (>90%), we determine that $LiAlH_4$ has the highest practical energy density and down-select it for further experimental work. Tests were performed in a vapor-hydrolysis reactor with three particle sizes (5 μm, 20 μm, and 50 μm diameter) and at three initial void fractions (86%, 71%, and 43%). We find that void fraction and particle size strongly affect reaction rates, but have no impact on reaction yields (all were ~100%) within the range tested. Higher void fraction and smaller particle size are correlated with faster reaction rates.

We find an unexpected mass accumulation in the hydride reaction products which attribute to hydrated lithium hydroxide formation, which affects void fraction and reaction rate. This reaction and its impact on reaction rate and yield in MFCs, and will need to be considered when designing an optimal pellet configuration.

Tests were performed in an MFC at 1.2 V constant potential discharge with $LiAlH_4$ at three particle sizes (5 μm, 20 μm, 50 μm) at a 32% initial void fraction. Consistent with the tests conducted in the hydrolysis reactor, the tests in the MFC show the strong impact of particle size on reaction rates, while reaction rates decrease with increasing particle size. Reaction yields were lower (90–93%) for the tests in the MFC, which attribute to a small hydrogen leak. The 93% yield corresponds to an energy density of 1003 Wh L^{-1} for the 7.7 cc MFC with 2.45 g of $LiAlH_4$, the highest reported to date.

Further work will be required to understand the impact of higher initial void fraction and lithium hydroxide hydrate formation on reaction rate and energy density. This data would enable development of optimal fuel pellet design, which would further improve the energy density of the MFC.

Acknowledgments

This material is based upon work supported by Honeywell International. Any opinions, findings and conclusions or recommendations expressed in this material are those of the authors and do not necessarily reflect the views of Honeywell International.

References

[1] H.I. Schlesinger, H.C. Brown, A.E. Finholt, J.R. Gilbreath, H.R. Hoekstra, E.K. Hyde, J. Am. Chem. Soc. 75 (1953) 215–219.
[2] W.D. Davis, L.S. Mason, G. Stegeman, J. Am. Chem. Soc. 71 (1949) 2775–2781.
[3] V.C.Y. Kong, F.R. Foulkes, Int. J. Hydrogen Energy 24 (1999) 665–675.
[4] V.C. Kong, D.W. Kirk, F.R. Foulkes, J.T. Hinatsu, Int. J. Hydrogen Energy 28 (2003) 205–214.
[5] C. Maupoix, J.L. Houzelot, E. Sciora, J. Powder Technol. 208 (2011) 318–323.
[6] S. Eickhoff, R. Wood, US Patent 7901816, 8 March 2011.
[7] Steven Eickhoff, AMPGen Quarterly Status Report. DARPA MTO MEMS PI Meeting (December 2004).
[8] S. Eickhoff, C. Zhang, T. Cui, J. Power Sources 240 (2013) 1–7.
[9] L. Zhu, V. Swaminathan, B. Gurau, R.I. Masel, M.A. Shannon, J. Power Sources 192 (2009) 556–561.
[10] I.H. MacPherson, Hydride as a Storage Medium. HIC Report (1992).
[11] L.H. Thomas, D.J. Holve, Part. Part. Syst. Charact. 10 (1993) 262–265.
[12] Y. Kojima, K.-I. Suzuki, Y. Kawai, J. Mater. Sci. 39 (2004) 2227–2229.